

Characterization of the FtsZ-Interacting Septal Proteins SepF and Ftn6 in the Spherical-Celled Cyanobacterium *Synechocystis* Strain PCC 6803[∇]

Martial Marbouty,¹ Cyril Saguez,¹ Corinne Cassier-Chauvat,^{1,2*} and Franck Chauvat^{1*}

CEA, iBiTec-S, SBIGeM, LBI, Bat 142 CEA-Saclay, F-91191 Gif sur Yvette CEDEX, France,¹ and CNRS, URA 2096, F-91191 Gif sur Yvette CEDEX, France²

Received 4 June 2009/Accepted 24 July 2009

Assembly of the tubulin-like cytoskeletal protein FtsZ into a ring structure at midcell establishes the location of the nascent division sites in prokaryotes. However, it is not yet known how the assembly and contraction of the Z ring are regulated, especially in cyanobacteria, the environmentally crucial organisms for which only one FtsZ partner protein, ZipN, has been described so far. Here, we characterized SepF and Ftn6, two novel septal proteins, in the spherical-celled strain *Synechocystis* PCC 6803. Both proteins were found to be indispensable to *Synechocystis* sp. strain PCC 6803. The depletion of both SepF and Ftn6 resulted in delayed cytokinesis and the generation of giant cells but did not prevent FtsZ polymerization, as shown by the visualization of green fluorescent protein (GFP)-tagged FtsZ polymers. These GFP-tagged Z-ring-like structures often appeared to be abnormal, because these reporter cells respond to the depletion of either SepF or Ftn6 with an increased abundance of total, natural, and GFP-tagged FtsZ proteins. In agreement with their septal localization, we found that both SepF and Ftn6 interact physically with FtsZ. Finally, we showed that SepF, but not Ftn6, stimulates the formation and/or stability of FtsZ polymers in vitro.

Binary fission of a mother cell to form two daughter cells is a widely conserved cell proliferation mechanism. In nearly all bacteria, cell division is initiated by the polymerization into a ring-like structure at midcell of the tubulin homolog GTPase protein FtsZ, which is also found in some archaea, as well as in plastids and some mitochondria (for reviews, see references 7, 21, and 33). The Z-ring is subsequently used as a scaffold for recruitment of downstream factors that execute the synthesis of the division septum. The assembly of this complex, also referred to as the divisome, has been thoroughly investigated in studies of the rod-shaped model organisms *Escherichia coli* and *Bacillus subtilis* (for reviews, see references 3, 4, 7, 9, 11, 19, and 21). In *E. coli*, more than 10 different proteins are required for the progression and completion of cell division. They are designated Fts proteins because their depletion leads to filamentation of the bacteria, and they are recruited to the division site in the following sequential order: FtsZ→FtsA/ZipA/ZapB→FtsK→FtsQ and FtsL/FtsB→FtsW→FtsI and FtsN.

The stability of the FtsZ protofilaments is thought to be important for assembly of the septal Z ring. Four FtsZ-interacting proteins have been shown to promote FtsZ polymerization and/or Z-ring stabilization, namely, ZapA and ZipA (found only in gammaproteobacteria), FtsA (an actin-like protein), and SepF (not found in gammaproteobacteria) (10, 31).

Both FtsA and ZipA assemble at the Z-ring early and participate in its anchorage to the inner face of the cytoplasmic membrane of the cell. They also participate in the recruitment of the downstream cytokinetic factor FtsK. Subsequently, the recruitment of FtsQ and the FtsB/FtsL complex allow the progressive assembly of downstream factors (FtsW, FtsI, and FtsN) involved in synthesis of the septal cell wall (7).

By contrast, the negative regulatory proteins MinCDE, DivIVA, EzrA, SulA, and Noc operate in the destabilization and positioning of the Z-ring at midcell (7, 21, 30), sometimes through a direct interaction with FtsZ (SulA, MinC, and ErzA).

Little is known concerning cell division in cyanobacteria, in spite of their crucial importance to the biosphere (5, 27, 34) and their interest for biotechnologists (1, 6, 32). Cyanobacteria are also attractive because many species (such as *E. coli* and *B. subtilis*) exhibit a cylindrical morphology with a well-defined middle, whereas many others have a spherical shape (29) and thus possess an infinite number of potential division planes at the point of greatest cell diameter. Furthermore, as the progenitor of the chloroplasts (8), cyanobacteria can be of help for deciphering the stromal chloroplastic division machinery (33). Interestingly, several cell division factors occurring in *E. coli* and *B. subtilis* have been shown (FtsZ, MinCDE, and SulA) or proposed (FtsE, FtsI, FtsQ, and FtsW) to be conserved in cyanobacteria (23, 26) and chloroplasts (which lack MinC) (33). In contrast, *ftsA*, *ftsB*, *zipA*, *ftsK*, *ftsL*, *ftsN*, and *zapA* have not been detected in cyanobacteria.

So far, cyanobacterial cytokinesis has mainly been investigated using the two unicellular species *Synechococcus* sp. strain PCC 7942 (rod shaped; hereafter *S. elongatus*) and *Synechocystis* sp. strain PCC 6803 (spherical-celled; hereafter *Synechocystis* sp.) and the filamentous strain *Anabaena* PCC 7120, all of which possess a fully sequenced genome (<http://genome.kazusa.or.jp/cyanobase/>) that is easily manipulated (16). Both FtsZ

* Corresponding author. Mailing address for Franck Chauvat: CEA, iBiTec-S, SBIGeM, LBI, Bat 142 CEA-Saclay, F-91191 Gif sur Yvette CEDEX, France. Phone: (33) 1 69 08 78 11. Fax: (33) 1 69 08 47 12. E-mail: franck.chauvat@cea.fr. Mailing address for Corinne Cassier-Chauvat: CEA, iBiTec-S, SBIGeM, LBI, Bat 142 CEA-Saclay, F-91191 Gif sur Yvette CEDEX, France. Phone: (33) 1 69 08 35 74. Fax: (33) 1 69 08 47 12. E-mail: corinne-cassier.chauvat@cea.fr.

[∇] Published ahead of print on 31 July 2009.

TABLE 1. Characteristics of the plasmids used in this study

Plasmid	Relevant feature(s) ^a	Source or reference
pGEMT	AT overhang Amp ^r cloning vector	Promega
pUC4K	Source of the Km ^r marker gene	Pharmacia
psepF	pGEMT with the <i>Synechocystis sepF</i> gene (slr2073) and flanking sequences where part of the SepF CS (from 186 to 426 bp) was replaced by a SmaI site	This study
pΔsepF::Km ^r	psepF with the Km ^r marker inserted into the unique SmaI site	This study
pFtn6	pGEMT with the <i>Synechocystis Ftn6</i> gene (sll1939) and flanking sequences where part of the Ftn6 CS (from 33 to 609 bp) was replaced by a SmaI site	This study
pΔftn6::Km ^r	pftn6 with the Km ^r marker inserted in the unique SmaI site	This study
pSBT	Km ^r Sm ^r Sp ^r plasmid replicating in <i>Synechocystis</i> sp. and expressing any gene cloned downstream of its <i>E. coli tac</i> promoter	22
pSM	pSBT derivative lacking the 1.349-kb SmaI segment carrying the Km ^r gene; all studied genes were cloned as blunt-end DNA segments downstream of its <i>tac</i> promoter at the unique SmaI site	This study
pC-GFP	Source of the enhanced GFP	23
pSZ-GFP	pSBT producing the <i>Synechocystis</i> FtsZ protein tagged with GFP	23
pSM-SepF	pSM producing the <i>Synechocystis</i> SepF protein	This study
pSM-GFP-SepF	pSM producing the GFP-SepF protein	This study
pSM-Ftn6	pSM producing the <i>Synechocystis</i> Ftn6 protein	This study
pSM-GFP-Ftn6	pSM producing the GFP-Ftn6 protein	This study
pCZ	Amp ^r Km ^r <i>E. coli</i> plasmid producing the <i>Synechocystis</i> FtsZ protein tagged with a six-His tag at its C terminus	23
pET28b(+)	Km ^r <i>E. coli</i> expression vector with T7 and LacO promoters with T7 and six-His tags added and including LacI gene	Novagen
p28-SepF	pET28b(+) harboring the SepF CS (with its own stop codon) cloned between the NdeI-BamHI sites	This study
p28-Ftn6	pET28b(+) harboring the Ftn6 CS (with its own stop codon) cloned between the NdeI-BamHI sites	This study
p28-GFP-SepF	pET28b(+) harboring the GFP-SepF translational fusion cloned between the NdeI-BamHI sites	This study
p28-GFP-Ftn6	pET28b(+) harboring the GFP-Ftn6 translational fusion cloned between the NdeI-BamHI sites	This study

^a CS, protein coding sequence; Δ, deletion.

and ZipN/Ftn2/Arc6, a protein occurring only in cyanobacteria (ZipN [alternative name, Ftn2]) and plant chloroplasts (Arc6), were found to be crucial for cytokinesis (17, 23, 26) and to physically interact with each other (20, 23). We also reported that the MinCDE system participates in determining the correct positioning of the septal Z ring at midcell (23). In addition, it has recently been shown in studies of *Synechococcus* sp. that inactivation of both the *cdv2* gene (an orthologue of the gene encoding *B.subtilis* sepF) and the *ftn6* gene (present in only some cyanobacteria) promotes filamentation, though their role in cell division has yet to be characterized (16, 26).

In a continuous effort to characterize the divisome machine of *Synechocystis* sp., we have used a combination of in vivo and in vitro techniques for thorough analysis of the SepF and Ftn6 proteins. We report here that both SepF and Ftn6 are crucial cytokinetic proteins that localize at the division site at midcell and whose depletion leads to the formation of giant cells that remain spherical. In agreement with their septal localization, both SepF and Ftn6 were found to interact physically with FtsZ; also, SepF, but not Ftn6, was found to stimulate the formation and/or stability of FtsZ polymers.

MATERIALS AND METHODS

Bacterial strains, growth, plasmids, and gene transfer procedures. *Synechocystis* sp. strain PCC 6803 was grown and transformed at 30°C in BG11 medium (29) enriched with 3.78 mM Na₂CO₃ under conditions of continuous white light of standard fluence (2,500 lx; 31.25 μE m⁻² s⁻¹) as described in reference 2. *E. coli* strains TOP10 (Invitrogen), CM404, and BL21(DE3), grown at 30°C (strain CM404) or 37°C (other strains) on LB with or without 1% glucose, were used for gene manipulation (strain TOP10), protein production (strain BL21), or conjugative transfer (25) to *Synechocystis* sp. (CM404) of the plasmids derived from the pSBTlac expression vector that replicates at about 10 copies per cell (i.e., one copy per chromosome copy) and expresses the studied genes from the *E. coli tac*

promoter (22). The selective antibiotics and final concentrations were as follows: for *E. coli*, ampicillin (Ap) at 100 μg ml⁻¹, kanamycin (Km) at 50 μg ml⁻¹, and spectinomycin (Sp) at 100 μg ml⁻¹; and for *Synechocystis* sp., Km at 50 to 300 μg ml⁻¹, streptomycin (Sm) at 5 μg ml⁻¹, and Sp at 2.5 to 10 μg ml⁻¹.

Gene cloning and DNA manipulations. All *Synechocystis* genes, surrounded by their flanking regions (about 300 bp) for homologous recombinations mediating targeted gene replacement in *Synechocystis* sp. (18), were amplified from wild-type (WT) DNA by PCR, using specific primers. After cloning was carried out with the appropriate plasmids (Table 1), site-directed mutagenesis was performed and disruptions were made through standard PCR-driven overlap extension (12). We used deletion cassettes that carry the antibiotic resistance marker inserted in the same orientation as the gene to be inactivated. The PCR-amplified protein-coding sequences were tagged with six-His through cloning into the *E. coli* expression vector pET28b(+) (Table 1) before or after fusion with the green fluorescent protein (GFP) sequence performed using overlapping PCR and were cloned into the NheI-NotI sites of pET28b(+). All constructions were verified by PCR and DNA sequencing (BigDye kit; ABI Perkin Elmer).

Light and fluorescence microscopy. *Synechocystis* cells (1.25 × 10⁵) from a mid-log-phase culture were placed on microscope slides and immobilized by 5 to 10 min of incubation at room temperature. Images were captured using a Leica DMRXA microscope equipped with a ×100 oil immersion lens, a Roper Scientific Micromax cooled charge-coupled-device camera, and Metamorph software (Universal Imaging). The final processing of images for presentation was done using Adobe Photoshop.

Fluorescence-activated cell sorter analysis. Cells from mid-log-phase liquid cultures were harvested, washed twice, and resuspended in phosphate-buffered saline (Sigma-Aldrich) to a final optical density at 580 nm of 0.3 (1.5 × 10⁷ cells ml⁻¹). Then, 2 × 10⁴ cells were analyzed by using a FACSCalibur cytometer (Becton Dickinson) with the following settings: forward scatter (FSC), E01 log; side scatter, 350 V. Results were collected with CellQuest software, version 3.1 (Becton Dickinson). Data were plotted on a two-dimensional graph (*x* axis, FSC; *y* axis, number of cells). Then, histograms from WT and mutant strains were superimposed. Experiments were repeated twice.

Protein production and purification. Recombinant *E. coli* BL21 cells were grown at 37°C for 2 h (to an optical density at 600 nm of 0.5 to 0.7) prior to induction with IPTG (1 mM isopropyl-β-D-thiogalactopyranoside) for 16 h at 28°C. Cells were harvested by centrifugation for 10 min at 5,000 rpm, washed with lysis buffer (50 mM Tris-HCl [pH 8.0], 300 mM NaCl, 5 mM imidazole),

resuspended for 5 min in ice-cold lysis buffer containing 2 mM phenylmethylsulfonyl fluoride, and subsequently incubated with lysozyme (1 mg/ml^{-1}) for 1 h on ice. Cells were disrupted by ultrasonication with three pulses of 30 s each. The lysate was cleared by centrifugation at $12,000 \times g$ for 30 min at 4°C . Six-His-tagged proteins were overexpressed and purified (23) on nickel-nitrilotriacetic acid agarose beads (Invitrogen), washed extensively with lysis buffer containing 25 mM imidazole, and eluted with lysis buffer containing 150 to 300 mM imidazole. Fractions containing the recombinant proteins were pooled and dialyzed against 50 mM Tris-HCl (pH 8.0)–5% (wt/vol) glycerol–300 mM NaCl. The purified proteins were concentrated using Amicon Ultra PL-10 (Millipore) at 4°C , quantified (Bio-Rad protein assay), aliquoted, and stored at -80°C until use. Proteins were estimated by sodium dodecyl sulfate-polyacrylamide gel electrophoresis (SDS-PAGE) to be $\geq 97\%$ pure (data not shown).

In vitro analysis of FtsZ interaction with GFP-tagged proteins. Analyses of interactions between preassembled FtsZ polymers and the GFP-tagged SepF or Ftn6 proteins were done as described previously (23). The polymers were visualized by phase-contrast microscopy and fluorescence microscopy.

Sedimentation assay. Analysis of the influence of both SepF and Ftn6 on the polymerization of FtsZ (as determined by the quantity of FtsZ-sedimentable mass) was performed essentially as described previously (31). Purified FtsZ ($4.5 \mu\text{M}$) was polymerized in assembly buffer (50 mM Tris [pH 7.5], 150 mM NaCl) for 30 min on ice in the presence of various concentrations (0, 2, 3, and $4 \mu\text{M}$) of either SepF or Ftn6. Then, 10 mM MgCl_2 and 1 mM GTP were added to the reaction mixture, which was then incubated for an additional 20 min at 37°C , and FtsZ polymers were sedimented by centrifugation at $28,000 \times g$ for 30 min at 30°C . The pellets were dissolved in 100 μl of SDS loading buffer and heated at 95°C for 5 min. Samples (20 μl) were subjected to electrophoresis using SDS-PAGE (12%), blotted onto a nitrocellulose membrane, and probed with anti-His tag (MAb 4A12E4; Invitrogen). Secondary M680 antibodies (Odyssey) were used to detect FtsZ and SepF or Ftn6 proteins. Images were obtained using an infrared scanner (Odyssey).

RESULTS

The depletion of both of the indispensable *Synechocystis* SepF and Ftn6 proteins leads to formation of giant cells. The *Synechocystis* genome (14) encodes two proteins, Slr2073 and Sll1939 (CyanoBase; <http://genome.kazusa.or.jp/cyanobase>), that share significant homology with the *Synechococcus* Ftn6 and Cdv2 proteins that are required for formation of cells of normal size (26). Indeed, both of the *Synechococcus* mutants lacking Ftn6 or depleted with respect to Cdv2 (an indispensable protein in this organism) exhibited a filamentous phenotype and displayed enlarged cells (17, 26). Also interesting is that whereas Ftn6 was detected in only some cyanobacteria (26), Cdv2 was found to be significantly homologous to the SepF protein of *B. subtilis* that stimulates FtsZ assembly by binding along its length (10, 31).

To investigate the effect of the presence of SepF and Ftn6 on the morphology and cytokinesis of *Synechocystis* sp., we constructed $\Delta\text{sepF}::\text{Km}^r$ and $\Delta\text{ftn6}::\text{Km}^r$ deletion cassettes (Table 1) in which each studied protein-coding sequence was replaced by the transcription-terminator-less Km-resistant (Km^r) marker for selection. After transformation in *Synechocystis* sp., which harbors about 10 chromosome copies per cell (18), we verified through PCR and DNA sequencing that the Km^r marker had properly replaced the studied gene; then, we assayed whether the segregation of WT and mutant chromosome copies was complete (i.e., whether the gene was dispensable to cell growth) or not (gene indispensable). All transformant clones invariably retained WT chromosome copies, even after several rounds of restreaking in the presence of increasing concentrations of Km to favor the amplification of the mutant chromosome copies (data not shown). These findings indicated that both the *sepF* and *ftn6* genes are essential to the

viability of *Synechocystis* sp. The SepF-depleted mutant ($\text{sepF}::\text{Km}^r/\text{sepF}^+$) appeared to grow slower than both the WT strain and the Ftn6-depleted ($\text{ftn6}::\text{Km}^r/\text{ftn6}^+$) mutant (doubling times about 19 h, 9 h, and 12 h, respectively).

Then, we inspected the cell morphology of these mutants through phase-contrast microscopy (Fig. 1). Both mutants, $\Delta\text{sepF}::\text{Km}^r/\text{sepF}^+$ and $\Delta\text{ftn6}::\text{Km}^r/\text{ftn6}^+$, displayed similar aberrant “giant” cell morphologies (45% and 31% of the cell populations, respectively; Fig. 1A), suggesting that cell division had somehow been caused to slow. The $\Delta\text{ftn6}::\text{Km}^r/\text{ftn6}^+$ mutant also displayed an increased amount of “doublet cells” compared to the WT strain (80% versus 60%), again suggesting that cell division had slowed. The global increase in cell size in the mutants compared to the WT strain was also confirmed using flow cytometry (Fig. 1B) by measuring the proportion of the FSC value to cell size (24). The mean FSC values were as follows: for the WT strain, 75.94; for $\Delta\text{sepF}::\text{Km}^r/\text{sepF}^+$ (noted as ΔsepF), 183.87; and for $\Delta\text{ftn6}::\text{Km}^r/\text{ftn6}^+$ (noted as Δftn6), 122.64.

To further confirm that both SepF and Ftn6 are important for normal cell size formation, we cloned the corresponding protein-coding sequences in our pSM plasmid (Table 1), a Km^s derivative of our previously constructed pSB2T expression vector (22), which harbors the *E. coli tac* promoter for expression of the studied gene and replicates autonomously at 10 copies per cell, i.e., 1 copy per chromosome copy (22). The resulting pSM-SepF and pSM-Ftn6 plasmids were transferred to *Synechocystis* sp., where they both modified cell morphology, as expected (Fig. 1). Indeed, both the WT/pSM-SepF and WT/pSM-Ftn6 reporter strains exhibited giant cells (28% and 33%, respectively), likely accounting for their high FSC mean values (123.12 and 119.17, respectively). Interestingly, the WT/pSM-Ftn6 mutant also displayed a total of 33% twisted (nonspherical) cells, a result not observed with the WT/pSM-SepF mutant.

Depletion of SepF and Ftn6 alters both the shape and the positioning of GFP-tagged FtsZ structures. One of the very important features of cytokinetic proteins is their role in assembly and/or positioning of the septal Z ring. For instance, no Z rings are formed at midcell in the absence of both FtsA and ZipA *E. coli* proteins (28) or after the depletion of the *Synechocystis* ZipN protein (23). To test the possible influence of the SepF and Ftn6 proteins on FtsZ structures, we introduced into the SepF- and Ftn6-depleted mutants the pSZ-GFP reporter plasmid (Table 1) we had previously used to visualize the septal Z ring at the middle of WT cells (23). In both SepF- and Ftn6-depleted cells, the FtsZ structures appeared to be localized at aberrant (ectopic) positions (Fig. 2) and, consistently, these reporter cells exhibited abnormal morphologies (occurrence of spiraled cells and excrescences) likely resulting from asymmetrical and/or incomplete septation. Collectively, these observations indicate that the depletion of both SepF and Ftn6 resulted in delayed cytokinesis and in the generation of giant cells but did not prevent FtsZ polymerization. That the GFP-tagged Z-ring-like structures appeared to be abnormal in these reporter cells resulted from the fact that they exhibit an increased abundance of FtsZ proteins due to the production of both natural and GFP-tagged FtsZ proteins after the depletion of either SepF or Ftn6.

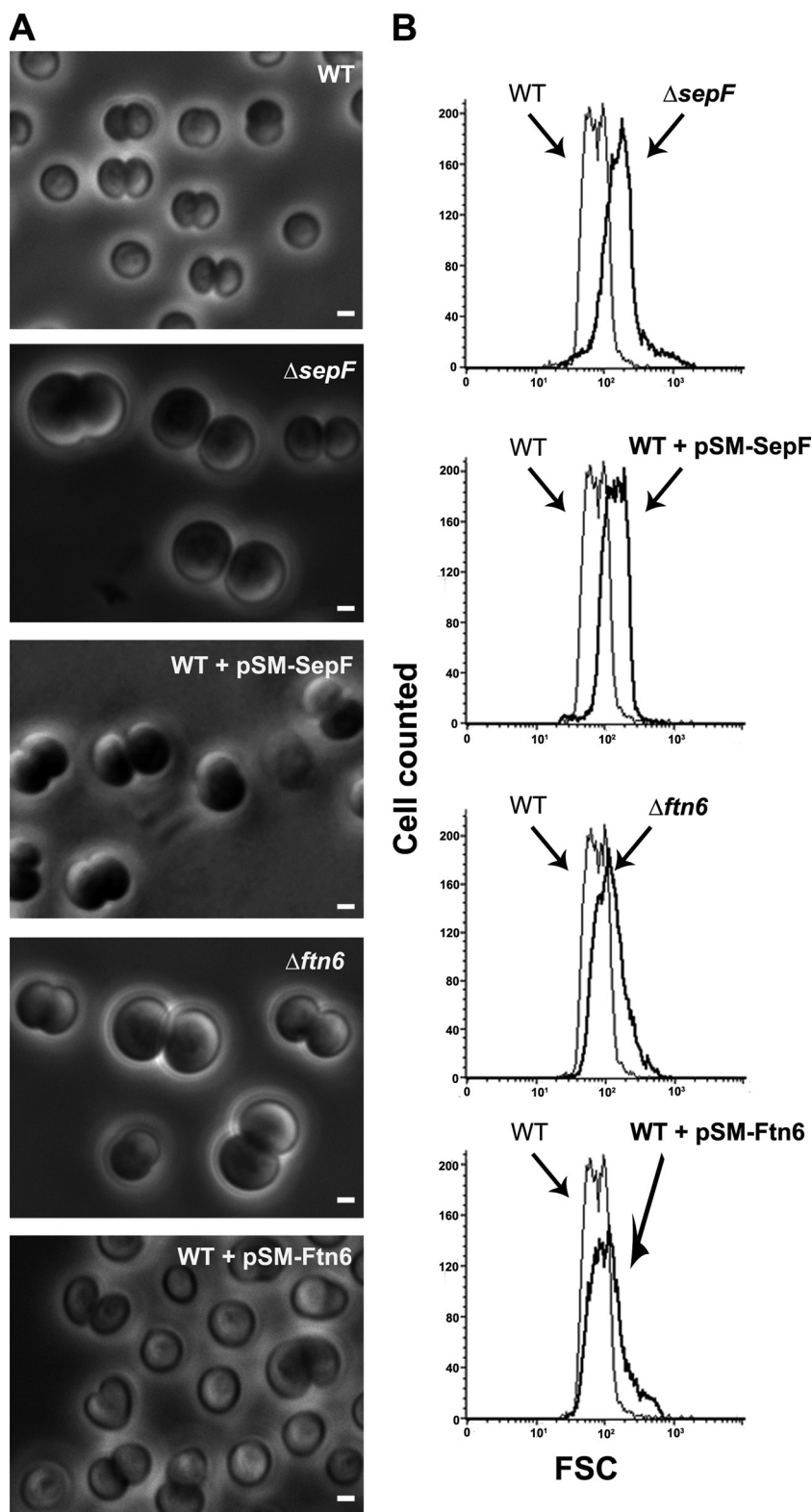


FIG. 1. Influence of the abundance of SepF and Ftn6 proteins on the morphology and size of *Synechocystis* cells. Phase-contrast image (A) (scale bars, 1 μ m) and flow cytometry analysis (B) of WT or mutant cells depleted with respect to (Δ) or producing the natural or tagged versions of the studied proteins from a pSM expression plasmid (Table 1). For each mutant strain, the FSC histogram (bold lines) has been overlaid with that of the WT to better visualize the influence of the mutation on cell size. These experiments were performed twice with two independent clones harboring the same mutation.

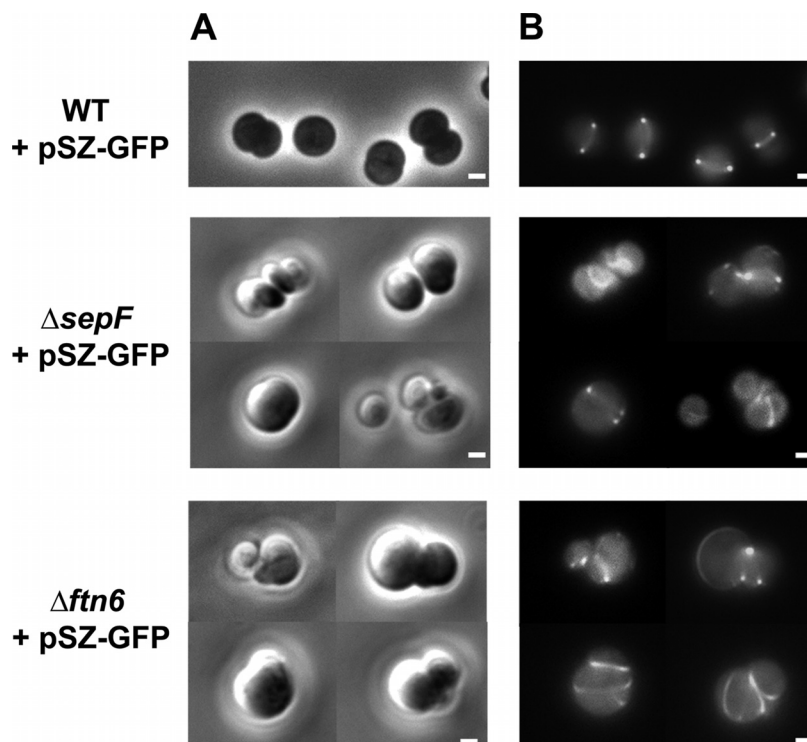


FIG. 2. Influence of the abundance of the protein SepF and Ftn6 on the structure and position of FtsZ networks. Phase-contrast images (A) (scale bars, 1 μ m) and corresponding fluorescence images (B) (scale bars, 1 μ m) of aberrant cells of different strains harboring the pSZ-GFP reporter plasmid (WT strain, $\Delta sepF::Km^r/sepF^+$ strain, and $\Delta ftn6::Km^r/ftn6^+$ strain) are shown.

Both GFP-SepF and GFP-Ftn6 proteins are biologically active and localize to the septum at midcell. To investigate the subcellular localization of the SepF and Ftn6 proteins, we translationally fused the coding sequence to the C terminus of the GFP and cloned the resulting fusion genes in pSM (Table 1), the $Sm^r Sp^r$ derivative of the expression vector we used to visualize the Z ring (23). The pSM-GFP-Ftn6 plasmid was introduced directly in the Ftn6-depleted strain ($\Delta ftn6::Km^r/ftn6^+$), where it restored a normal cell size (Fig. 3). This finding showed that the GFP-Ftn6 reporter protein is functional in that it is able to compensate for the depletion of the natural Ftn6 protein. Very interestingly, the fluorescent GFP-Ftn6 reporter protein exhibited a septal localization at midcell (Fig. 3).

The pSM-GFP-SepF $Sm^r Sp^r$ plasmid could not be directly introduced in the SepF-depleted cells, as demonstrated by the fact that they grew poorly. Alternatively, this plasmid was introduced in WT cells, generating the pSM-GFP-SepF reporter strain, which was subsequently transformed with the *sepF* deletion cassette $\Delta sepF::Km^r$, yielding the $\Delta sepF::Km^r/pSM-GFP-SepF$ reporter strain. These cells exhibited a normal cell morphology, unlike the SepF-depleted $\Delta sepF::Km^r/sepF^+$ cells (Fig. 3), showing that the GFP-SepF reporter protein is biologically active in compensating for SepF depletion. In similarity to GFP-Ftn6, the GFP-SepF reporter protein exhibited a septal localization at the midcell (Fig. 3). Collectively, these findings indicate that both Ftn6 and SepF are targeted to the septum, where they might physically interact with FtsZ.

Both GFP-SepF and GFP-Ftn6 proteins can bind to FtsZ polymers preassembled in vitro. As we found that both the GFP-SepF and GFP-Ftn6 proteins are targeted to the septum at the midcell (Fig. 3), we tested whether they can physically interact with FtsZ. For this purpose, we used our previously published in vitro assay, taking advantage of the self-assembly of FtsZ into polymers, which can be subsequently decorated by a GFP-tagged FtsZ partner protein (23). Hence, preformed FtsZ polymers were incubated with the proteins six-His-GFP-SepF, six-His-GFP-Ftn6, and six-His-GFP (negative control; see reference 23) and subsequently examined using optical and fluorescence microscopy. The FtsZ filaments became highly fluorescent following incubation with six-His-GFP-SepF and six-His-GFP-Ftn6 (Fig. 4) but not after incubation with six-His-GFP (negative control). These findings show that both the SepF protein and the Ftn6 protein are able to interact with FtsZ polymers in vitro.

SepF, but not Ftn6, stimulates assembly and/or stability of FtsZ polymers in vitro. To test the influence of both SepF and Ftn6 on FtsZ assembly, we performed an in vitro polymerization assay of FtsZ in the presence of increasing concentrations of either SepF or Ftn6. FtsZ polymers were purified by sedimentation, and their quantities were estimated by both Coomassie blue staining (data not shown) and Western blot analysis using antibodies directed against the six-His tag of all these studied proteins (Fig. 4). Interestingly, the amount of FtsZ converted into FtsZ polymers increased in parallel with the concentration of SepF not with that of Ftn6. These findings

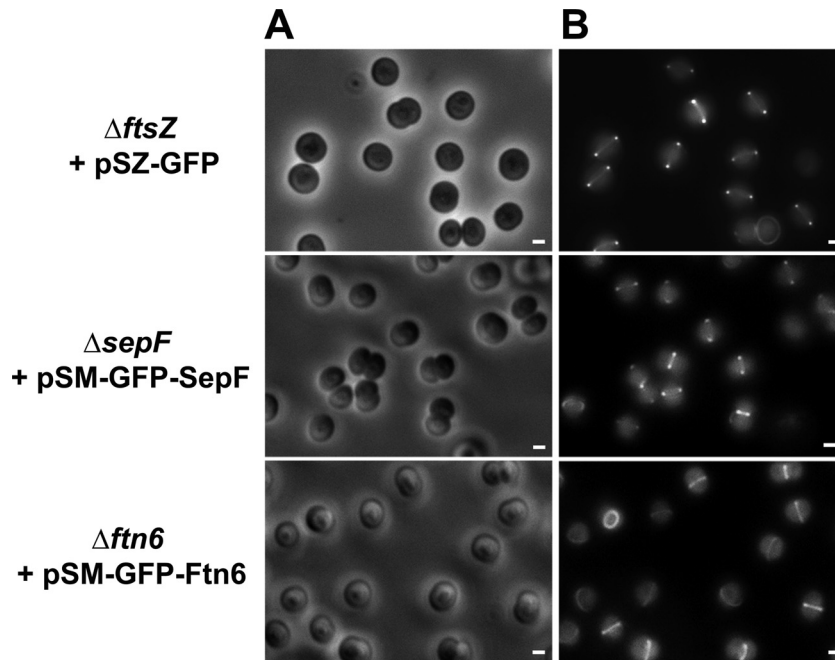


FIG. 3. Localization of proteins SepF and Ftn6 at the septum. Phase-contrast images (A) (scale bars, 1 μm) and corresponding fluorescence images (B) (scale bars, 1 μm) of indicated strains ($\Delta\text{ftsZ}::\text{Km}^r$ + pSZ-GFP, $\Delta\text{sepF}::\text{Km}^r$ + pSM-GFP-SepF, and $\Delta\text{ftn6}::\text{Km}^r$ + pSM-GFP-Ftn6) are shown.

indicate that SepF, but not Ftn6, stimulates FtsZ polymerization or stabilizes the polymers.

DISCUSSION

As very little is known concerning cell division in the environmentally crucial cyanobacteria, we have thoroughly investigated Ftn6 and SepF, the two cytokinetic proteins, in studies of the widely used unicellular cyanobacterium *Synechocystis* sp. strain PCC 6803.

SepF has been well characterized in studies of the rod-shaped bacterium *B. subtilis*, where it was found to be a septal protein and to physically interact with FtsZ (10), thereby promoting assembly and bundling of FtsZ protofilaments (31). In studies of cyanobacteria, analysis of SepF has been initiated using the rod-shaped unicellular strain *Synechococcus* sp. strain PCC 7942, and it has been found that its depletion generated double-length cells responsible for the filamentous morphology of the corresponding *cdv2* mutant (26). As seen with *Synechococcus* sp., we found SepF to be essential to cell viability in *Synechocystis* sp. and to participate in the formation of cells of normal size (Fig. 1). In both of these cyanobacterial species, SepF depletion generated giant cells that retained their overall morphology, i.e., cylindrical morphology in *Synechococcus* sp. (26) and spherical morphology in *Synechocystis* sp. (Fig. 1). Going deeper into the role of the SepF in cyanobacteria, we found that SepF is targeted to the *Synechocystis* septum at midcell (Fig. 3), where it likely interacts with FtsZ. Supporting this assumption, we showed that SepF can indeed bind to FtsZ polymers preassembled *in vitro* and that SepF stimulates assembly and/or stability of FtsZ polymers (Fig. 4), as occurs in *B. subtilis*. These findings are important, as they

show that not only the presence but also the function of a cytokinetic factor can be well conserved in prokaryotes, even in those that differ in the following important aspects: metabolism (photoautotrophy in cyanobacteria versus heterotrophy in *B. subtilis*), cell envelopes (gram negative in cyanobacteria versus gram positive in *B. subtilis*), and morphology (spherical in *Synechocystis* sp. versus cylindrical in *B. subtilis*).

Ftn6, a cyanobacterium-specific cytokinetic factor, was first identified in the rod-shaped unicellular strain *Synechococcus* PCC7942. It has been termed Ftn6 because its absence results in longer cells responsible for the filamentous morphology of the *ftn6*-deletion mutant (17, 26). This observation is reminiscent of what occurs in two intensively studied cylindrical bacteria, *E. coli* and *B. subtilis*, for which a wealth of mutants altered in cytokinesis are filamentous (for reviews, see reference 3 and references 4, 7, 9, 11, 19, and 21). The simplest explanation for this phenotype is that the frequency of complete septation decreases while cell growth, i.e., the lateral insertion of the peptidoglycan, continues (13). With respect to spherical cyanobacteria such as *Synechocystis* sp., for which the consequences for cell morphology of mutations slowing down septation more strongly than cell growth have not been well documented, we believe that such mutations should give rise to giant cells that remain spherical. As is consistent with this hypothesis, we report here that the depletion of either Ftn6 or SepF resulted in the generation of giant cells that remained spherical (Fig. 1). As seen with SepF, Ftn6 was found to be crucial to cell viability in *Synechocystis* sp. whereas it is dispensable in *Synechococcus* sp. (17, 26). The reason for this discrepancy between the two cyanobacteria is unclear, but this finding emphasizes the importance of parallel studies of cell

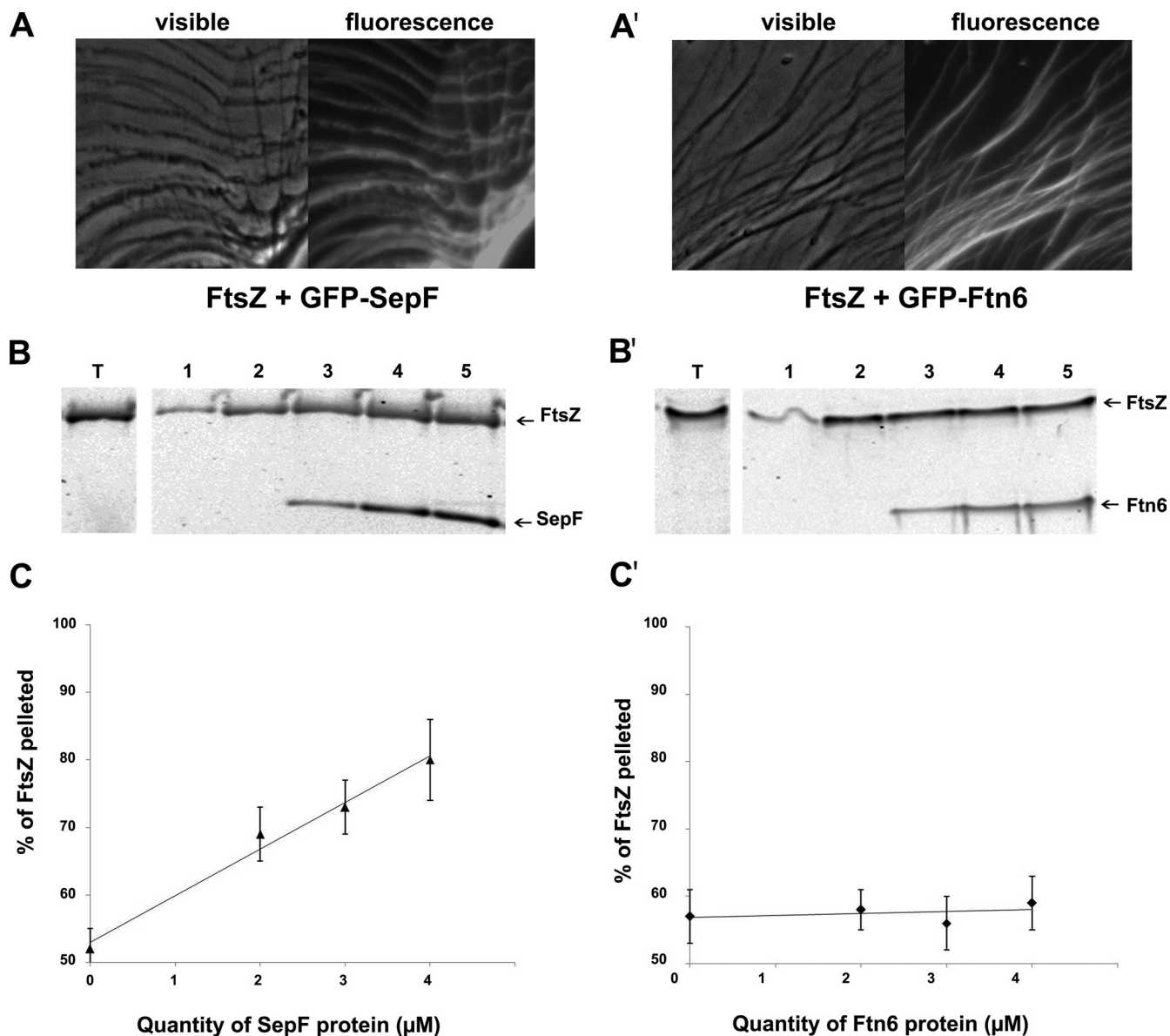


FIG. 4. Both SepF and Ftn6 interact with FtsZ, and SepF but not Ftn6 stimulates assembly and/or stability of FtsZ polymers. Phase-contrast images and corresponding fluorescence images showing that GFP-SepF (A) and GFP-Ftn6 (A') decorate the FtsZ polymer network are presented. Effects of SepF (B and C) and Ftn6 (B' and C') on the sedimentable polymeric mass of FtsZ are shown. FtsZ (4.5 μ M) was polymerized in the absence or presence of different concentrations of SepF or Ftn6, and the polymers were collected by centrifugation. The protein content in the pellets were visualized by Western blotting using anti-His tag antibodies (B and B') and then quantified (C and C') as described in Materials and Methods. Lanes T represent the total amount of FtsZ used for the experiment, which was performed twice. Results show data representing the polymeric mass obtained when FtsZ was incubated without GTP (lanes 1) or with 1 mM GTP (lanes 2 to 5) in the absence (lanes 2) or in the presence of 2 μ M (lanes 3), 3 μ M (lanes 4), and 4 μ M (lanes 5) concentrations of either SepF (B and C) or Ftn6 (B' and C').

division in both spherical organisms (such as *Synechocystis* sp.) and cylindrical organisms (such as *Synechococcus* sp.).

Ftn6 was found to be targeted to the septum at the midcell and, consistently, to physically interact with *in vitro*-preassembled FtsZ polymer, as seen with SepF (Fig. 4). Again, as observed for SepF, the depletion of Ftn6 did not prevent FtsZ polymerization. That the Z ring-like structures often appeared to be abnormal in the Ftn6- and SepF-depleted mutants was likely due to the fact that the cells respond to the depletion of either Ftn6 or SepF with an increased abundance of FtsZ

proteins due to the production of both GFP-tagged and untagged FtsZ proteins. However, unlike SepF, Ftn6 was not found to stimulate the assembly and/or stability of FtsZ polymers (Fig. 4).

Although SepF and Ftn6 exhibit similar depletion phenotypes, namely, septal localization and interaction with FtsZ, it is unlikely that they share the same overlapping functions. Indeed, the Ftn6-overproduction mutant displayed a total of 33% twisted (nonspherical) cells, a result not observed in the SepF-overproduction mutant (Fig. 1). In addition, SepF, but

not Ftn6, was found to stimulate assembly and/or stabilization of Z-polymers (Fig. 4). Altogether, our data suggest that Ftn6 acts of downstream of SepF, i.e., in the location after the assembly of the Z ring.

In conclusion, both SepF and Ftn6 are new FtsZ-interacting septal proteins in cyanobacteria, for which only one such protein, ZipN, has been characterized so far (23). It will be especially interesting in the future to investigate the likely relations among these three septal proteins.

ACKNOWLEDGMENTS

M.M. and C.S. were recipients of Ph.D. and postdoctorate fellowships from the CEA (France).

REFERENCES

- Dismukes, G. C., D. Carrieri, N. Bennette, G. M. Ananyev, and M. C. Posewitz. 2008. Aquatic phototrophs: efficient alternatives to land-based crops for biofuels. *Curr. Opin. Biotechnol.* **19**:235–240.
- Domain, F., L. Houot, F. Chauvat, and C. Cassier-Chauvat. 2004. Function and regulation of the cyanobacterial genes *lexA*, *recA* and *ruvB*: LexA is critical to the survival of cells facing inorganic carbon starvation. *Mol. Microbiol.* **53**:65–80.
- Ebersbach, G., E. Galli, J. Moller-Jensen, J. Lowe, and K. Gerdes. 2008. Novel coiled-coil cell division factor ZapB stimulates Z ring assembly and cell division. *Mol. Microbiol.* **68**:720–735.
- Errington, J., R. A. Daniel, and D. J. Scheffers. 2003. Cytokinesis in bacteria. *Microbiol. Mol. Biol. Rev.* **67**:52–65.
- Ferris, M., and B. Palenik. 1998. Niche adaptation in ocean cyanobacteria. *Nature* **396**:226–228.
- Ghirardi, M. L., A. Dubini, J. Yu, and P. C. Maness. 2009. Photobiological hydrogen-producing systems. *Chem. Soc. Rev.* **38**:52–61.
- Goehring, N. W., and J. Beckwith. 2005. Diverse paths to midcell: assembly of the bacterial cell division machinery. *Curr. Biol.* **15**:R514–R526.
- Gray, M. W. 1993. Origin and evolution of organelle genomes. *Curr. Opin. Genet. Dev.* **3**:884–890.
- Haeusser, D. P., and P. A. Levin. 2008. The great divide: coordinating cell cycle events during bacterial growth and division. *Curr. Opin. Microbiol.* **11**:94–99.
- Hamoen, L. W., J. C. Meile, W. de Jong, P. Noirot, and J. Errington. 2006. SepF, a novel FtsZ-interacting protein required for a late step in cell division. *Mol. Microbiol.* **59**:989–999.
- Harry, E., L. Monahan, and L. Thompson. 2006. Bacterial cell division: the mechanism and its precision. *Int. Rev. Cytol.* **253**:27–94.
- Heckman, K. L., and L. R. Pease. 2007. Gene splicing and mutagenesis by PCR-driven overlap extension. *Nat. Protoc.* **2**:924–932.
- Justice, S. S., D. A. Hunstad, L. Cegelski, and S. J. Hultgren. 2008. Morphological plasticity as a bacterial survival strategy. *Nat. Rev. Microbiol.* **6**:162–168.
- Kaneko, T., S. Sato, H. Kotani, A. Tanaka, E. Asamizu, Y. Nakamura, N. Miyajima, M. Hirosawa, M. Sugiura, S. Sasamoto, T. Kimura, T. Hosouchi, A. Matsuno, A. Muraki, N. Nakazaki, K. Naruo, S. Okumura, S. Shimpo, C. Takeuchi, T. Wada, A. Watanabe, M. Yamada, M. Yasuda, and S. Tabata. 1996. Sequence analysis of the genome of the unicellular cyanobacterium *Synechocystis* sp. strain PCC 6803. II. Sequence determination of the entire genome and assignment of potential protein-coding regions. *DNA Res.* **3**:109–136.
- Reference deleted.
- Koksharova, O. A., and C. P. Wolk. 2002. Genetic tools for cyanobacteria. *Appl. Microbiol. Biotechnol.* **58**:123–137.
- Koksharova, O. A., and C. P. Wolk. 2002. A novel gene that bears a DnaJ motif influences cyanobacterial cell division. *J. Bacteriol.* **184**:5524–5528.
- Labarre, J., F. Chauvat, and P. Thuriaux. 1989. Insertional mutagenesis by random cloning of antibiotic resistance genes into the genome of the cyanobacterium *Synechocystis* strain PCC 6803. *J. Bacteriol.* **171**:3449–3457.
- Lutkenhaus, J. 2007. Assembly dynamics of the bacterial MinCDE system and spatial regulation of the Z ring. *Annu. Rev. Biochem.* **76**:539–562.
- Maple, J., C. Aldridge, and S. G. Moller. 2005. Plastid division is mediated by combinatorial assembly of plastid division proteins. *Plant J.* **43**:811–823.
- Margolin, W. 2005. FtsZ and the division of prokaryotic cells and organelles. *Nat. Rev. Mol. Cell Biol.* **6**:862–871.
- Marraccini, P., S. Bulteau, C. Cassier-Chauvat, P. Mermet-Bouvier, and F. Chauvat. 1993. A conjugative plasmid vector for promoter analysis in several cyanobacteria of the genera *Synechococcus* and *Synechocystis*. *Plant Mol. Biol.* **23**:905–909.
- Mazouni, K., F. Domain, C. Cassier-Chauvat, and F. Chauvat. 2004. Molecular analysis of the key cytokinetic components of cyanobacteria: FtsZ, ZipN and MinCDE. *Mol. Microbiol.* **52**:1145–1158.
- Meberg, B. M., A. L. Paulson, R. Priyadarshini, and K. D. Young. 2004. Endopeptidase penicillin-binding proteins 4 and 7 play auxiliary roles in determining uniform morphology of *Escherichia coli*. *J. Bacteriol.* **186**:8326–8336.
- Mermet-Bouvier, P., C. Cassier-Chauvat, P. Marraccini, and F. Chauvat. 1993. Transfer and replication of RSF1010-derived plasmids in several cyanobacteria of the genera *Synechocystis* and *Synechococcus*. *Curr. Microbiol.* **26**:323–327.
- Miyagishima, S. Y., C. P. Wolk, and K. W. Osteryoung. 2005. Identification of cyanobacterial cell division genes by comparative and mutational analyses. *Mol. Microbiol.* **56**:126–143.
- Partensky, F., W. R. Hess, and D. Vaultot. 1999. *Prochlorococcus*, a marine photosynthetic prokaryote of global significance. *Microbiol. Mol. Biol. Rev.* **63**:106–127.
- Pichoff, S., and J. Lutkenhaus. 2002. Unique and overlapping roles for ZipA and FtsA in septal ring assembly in *Escherichia coli*. *EMBO J.* **21**:685–693.
- Rippka, R., J. Deruelles, J. Waterbury, M. Herdman, and R. Stanier. 1979. Generic assignments, strains histories and properties of pure cultures of cyanobacteria. *J. Gen. Microbiol.* **111**:1–61.
- Singh, J. K., R. D. Makde, V. Kumar, and D. Panda. 2007. A membrane protein, EzrA, regulates assembly dynamics of FtsZ by interacting with the C-terminal tail of FtsZ. *Biochemistry* **46**:11013–11022.
- Singh, J. K., R. D. Makde, V. Kumar, and D. Panda. 2008. SepF increases the assembly and bundling of FtsZ polymers and stabilizes FtsZ protofilaments by binding along its length. *J. Biol. Chem.* **283**:31116–31124.
- Williams, P. G. 2009. Panning for chemical gold: marine bacteria as a source of new therapeutics. *Trends Biotechnol.* **27**:45–52.
- Yang, Y., J. M. Glynn, B. J. Olson, A. J. Schmitz, and K. W. Osteryoung. 2008. Plastid division: across time and space. *Curr. Opin. Plant Biol.* **11**:577–584.
- Zehr, J. P., J. B. Waterbury, P. J. Turner, J. P. Montoya, E. Omoregie, G. F. Steward, A. Hansen, and D. M. Karl. 2001. Unicellular cyanobacteria fix N₂ in the subtropical North Pacific Ocean. *Nature* **412**:635–638.